

# Time–frequency phase differences and phase locking to characterize dynamic interactions between cardiovascular signals

Michele Orini, Raquel Bailón, Luca T. Mainardi and Pablo Laguna

**Abstract**—In this paper cross time–frequency (TF) analysis is used to estimate the phase differences and the phase locking between cardiovascular signals. Phase differences give a measure of the changes in the synchronization between two oscillations, while phase locking measures the degree of similarity of these changes across subjects. The methodology is based on the smoothed pseudo Wigner–Ville distribution and includes coherence analysis. In a simulation study involving R–R variability (RRV) signals, this methodology provided accurate estimates of phase differences, with an error characterized by interquartile ranges lower than 2% and 10% for SNR of 20 dB and 0 dB, respectively. A comparative study showed that the proposed estimator outperformed an estimator based on the integration of the difference between the instantaneous frequencies of the signal spectral component. The presented methodology was used to characterize the interactions between RRV and systolic arterial pressure variability during tilt table test. Head-up tilt caused the phase differences (time delay) to change about 0.48 rad (361 ms) in HF range [0.15, 0.5 Hz]. The phase locking, which decreased immediately after the head-up tilt, was restored in about 2 minutes.

## I. INTRODUCTION

Short-term cardiovascular control involves homeostatic mechanisms which create a dynamic coupling between the the systolic arterial pressure and the heart period. An impairment of the cardiovascular regulation may alter the degree of synchronization of these signals. The time–frequency phase difference (TFPD) spectrum quantifies the changes in the synchronization between two oscillations, and the time–frequency phase locking (TFPL) measures the degree of similarity of these changes across subjects. These quantities can reveal valuable information to characterize the dynamic interactions between signals related to the cardiovascular control. An illustrative example of two synthetic signals which share similar instantaneous frequencies but with time–varying phase differences, is shown in Fig. 1. This example may represent LF oscillations of R–R variability (RRV) and systolic arterial pressure variability (SAPV) during non–stationary conditions. The estimation of the phase differences between non–stationary signals in the joint TF domain was used in few studies [1], [2]. Among them, no one focuses on the characterization of cardiovascular dynamics. From a methodological viewpoint, TFPD has been estimated by wavelet transform [2], by Rihaczek transform [1] and by

This work was supported by Ministerio de Ciencia y Tecnología, FEDER under Project TEC2010-21703-C03-02 and TRA2009-0127

M. Orini, P. Laguna and R. Bailón are with GTC, I3A, IIS Aragón, Universidad de Zaragoza and with CIBER–BBN, Zaragoza, Spain; michele@unizar.es

M. Orini and L.T. Mainardi are with Department of Bioengineering, Politecnico di Milano, Milan, Italy.

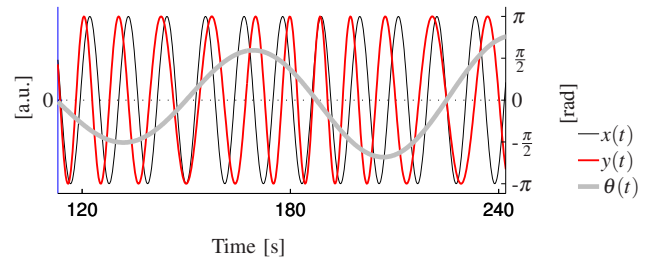


Fig. 1. Example of signals oscillating at typical Mayer wave frequency and characterized by time–varying phase differences  $\theta(t)$

reduced interference distributions [3].

The purpose of this study is to describe a robust technique to accurately estimate the TFPD and TFPL via smoothed pseudo Wigner–Ville distribution (SPWVD), and to show the usefulness of such approach in the analysis of cardiovascular control. The presented methodology is assessed in simulation studies and is used to characterize the dynamic interactions between RRV and SAPV signals during tilt table test.

## II. METHODS

Cardiovascular signals can be modeled as the real part of:

$$\begin{cases} x(t) = A_{x,LF}(t)e^{i\theta_{x,LF}(t)} + A_{x,HF}(t)e^{i\theta_{x,HF}(t)} + w_x(t) \\ y(t) = A_{y,LF}(t)e^{i\theta_{y,LF}(t)} + A_{y,HF}(t)e^{i\theta_{y,HF}(t)} + w_y(t) \end{cases} \quad (1)$$

where LF and HF indicate the low frequency component,  $LF \in [0.04, 0.15]$  Hz, and the high frequency component,  $HF \in [0.15, 0.4]$  Hz, respectively;  $\theta_{k,B}(t)$ , with  $B \in [LF, HF]$  and  $k \in [x, y]$ , is the instantaneous phase, related to the instantaneous frequency by  $f_{k,B}(t) = (d\theta_{k,B}(t)/dt)/(2\pi)$ ;  $w_k(t)$  is a Gaussian white noise (WGN). As cardiovascular signals are non–stationary, the phase differences between their spectral components,  $\theta_B(t) = \theta_{x,B}(t) - \theta_{y,B}(t)$ , are expected to be time–varying. Given (1), the time–course of the phase differences between the spectral component  $B$  of two signals can be estimated as:

$$\hat{\theta}_B(t) = 2\pi \int_0^t [f_{x,B}(\tau) - f_{y,B}(\tau)] d\tau \quad (2)$$

This procedure has two main drawbacks: it is very sensitive to estimation errors in  $f_{k,B}(t)$ , since an estimation error at  $t_0$  affects all  $\hat{\theta}_B(t > t_0)$ , and gives a quantification of the phase differences only at  $f_{k,B}(t)$ . In cardiovascular analysis, these inconveniences are particularly serious, since biomedical signals are never narrow–band and an accurate estimation of the instantaneous frequencies is not always possible.

Cross TF analysis provides a simultaneous characterization

of the phase differences in time and frequency, and allows to overcome these limitations. The presented methodology is based on the estimation of the TFPD spectrum, from which the time–courses of the phase differences are extracted. It is composed of the following steps:

(i) Estimation of auto and cross TF spectra,  $\hat{S}_{xx}(t,f)$ ,  $\hat{S}_{yy}(t,f)$  and  $\hat{S}_{xy}(t,f)$ , via SPWVD [4], [5]:

$$\hat{S}_{xy}(t,f) = \iint_{-\infty}^{\infty} \Phi(\tau, \nu) A_{xy}(\tau, \nu) e^{i2\pi(t\nu - f\tau)} d\nu d\tau \quad (3)$$

$$A_{xy}(\tau, \nu) = \int_{-\infty}^{\infty} x\left(t + \frac{\tau}{2}\right) y^*\left(t - \frac{\tau}{2}\right) e^{-i2\pi\nu t} dt \quad (4)$$

$$\Phi(\tau, \nu; \tau_0, \nu_0, \lambda) = \exp\left\{-\pi\left[\left(\frac{\nu}{\nu_0}\right)^2 + \left(\frac{\tau}{\tau_0}\right)^2\right]^{2\lambda}\right\} \quad (5)$$

where  $A_{xy}(\tau, \nu)$  is the cross ambiguity function and  $\Phi(\tau, \nu)$  is a smoothing kernel function, already used in cross time–frequency analysis of cardiovascular signals [5], [6], [7].

(ii) Estimation of the TFPD spectrum,  $\hat{\Theta}(t,f)$ , and TF coherence,  $\hat{\gamma}(t,f)$  [5], as:

$$\hat{\Theta}(t,f) = \arctan\left[\frac{\Im[\hat{S}_{xy}(t,f)]}{\Re[\hat{S}_{xy}(t,f)]}\right]; \quad \hat{\Theta}(t,f) \in [-\pi, \pi] \quad (6)$$

$$\hat{\gamma}(t,f) = \frac{|\hat{S}_{xy}(t,f)|}{\sqrt{\hat{S}_{xx}(t,f)\hat{S}_{yy}(t,f)}}; \quad \hat{\gamma}(t,f) \in [0, 1] \quad (7)$$

(iii) Localization of the TF regions where the coherence is statistically significant. This is done by a hypothesis test, based on the comparison of  $\hat{\gamma}(t,f)$  with a threshold function  $\gamma_{th}(t,f)$ , estimated as the 95<sup>th</sup> percentile of the statistical distribution  $\Gamma(t,f) = \{\hat{\gamma}_1(t,f), \dots, \hat{\gamma}_j(t,f), \dots\}$ , where  $\hat{\gamma}_j(t,f)$  is the TFC between the  $j$ th realization of two WGNs. The estimation of the threshold as the 95<sup>th</sup> percentile of  $\Gamma(t,f)$  is associated to a significance level (type I error) of 5%. A TF mask  $M(t,f)$  is defined which is equal to one if  $\hat{\gamma}(t,f) > \gamma_{th}(t,f)$  and zero otherwise. It localizes the regions where TF coherence is significant.

(iv) Identification of the TF region  $\Omega_B$  in which the time–courses of the phase differences are estimated, as:

$$\Omega_B = \left\{ (t,f) \in (\mathbb{R}^+ \times B) \mid [M(t,f) \circ C(t,f)] = 1 \right\} \quad (8)$$

with  $B \in \{LF, HF\}$  and where  $C(t,f)$  is a rectangle of sides  $2s \times 0.025$  Hz and  $\circ$  denotes the opening (processing technique which involves erosion and dilation).

(v) The time–course of the phase differences between the spectral components of two signals,  $\hat{\theta}_B(t)$ , are estimated (in radians) by averaging the TFPD spectrum in  $\Omega_B$ :

$$\hat{\theta}_B(t) = \left[ \int_{\Omega_B} \Theta(t,f) df \right] / \left[ \int_{\Omega_B} 1 df \right] \quad (9)$$

The time delay (given in seconds) associated to  $\hat{\theta}_B(t)$  is:

$$\hat{\theta}_B(t) = \hat{\theta}_B(t) / \left[ 2\pi \arg \max_{f \in \Omega_B} |\hat{S}_{xy}(t,f)| \right] \quad (10)$$

where the term in the denominator is the instantaneous angular frequency which corresponds to the maximum of

the cross spectrum in  $\Omega_B$ .

The degree of phase–locking between different couples of signals [1] is estimated, on the whole population, by the TFPL:

$$\hat{\Psi}(t,f) = \left| \frac{1}{L} \sum_{j=1}^L e^{i2\pi\hat{\Theta}_j(t,f)} \right|, \quad \hat{\Psi}(t,f) \in [0, 1] \quad (11)$$

where  $L$  is the number of subjects. For a given TF point,  $\hat{\Psi}(t,f)=1$  if at that point the phase differences are the same for all subjects, while  $\hat{\Psi}(t,f)=0$  if the phase differences randomly change across subjects.

### III. MATERIALS

#### A. Simulation studies

Simulation studies were carried on with the purpose of validating the proposed methodology and comparing its performance with a traditional estimator not based on cross TF analysis. The signals used in these simulations are modified versions of the RRV signals recorded during the tilt table test described in the following section. They are obtained as  $x(t) = a_{RRV}(t) + w_x(t)$  and  $y(t) = x(t)\exp(i\theta(t)) + w_y(t)$ , where  $a_{RRV}(t)$  is the complex analytic signal representation of the RRV signal, and  $w_k(t)$  are WGN. Two cases are simulated. In the first one,  $\theta(t)$  changes sinusoidally (see Fig. 2a, 2e), while in the second one  $\theta(t)$  changes quadratically (see Fig. 2b, 2f). The estimation of  $\theta_B(t)$  was performed via cross TF analysis as well as directly via the instantaneous frequency estimates as in (2), and it was repeated for different level of SNR, going from 20 to 0 dB.

#### B. Physiological study

Signals were recorded from 14 young healthy subjects (age  $29 \pm 3$  years) during a tilt table test with a protocol already illustrated in [6]. The experimental protocol consisted of: 4 minutes in early supine position ( $W_1$ ), 5 minutes head–up tilted to an angle of  $70^\circ$  ( $W_2$ ) and 4 minutes back to later supine position ( $W_3$ ). During head–up tilt, subjects undergo a progressive orthostatic stress. The ECG was recorded by using the BIOPAC MP 150 system with a sampling frequency of 1 kHz, while the pressure signal was recorded in the finger by the Finometer<sup>®</sup> system with a sampling frequency of 250 Hz. Beats from ECG and pulses from the pressure signal were detected to generate RR and systolic arterial pressure time series. The RR series was estimated as  $RR(n) = t_{n+1}^{QRS} - t_n^{QRS}$  and the systolic arterial pressure series  $SAP(n)$  was obtained as the maximum of the pressure signal within a short interval following  $t_n^{QRS}$ , where  $t_n^{QRS}$  is the time of occurrence of the  $n$ <sup>th</sup> QRS complex in the ECG. During the procedure, the Finometer<sup>®</sup> was recalibrated at the beginning of  $W_2$  and  $W_3$ . The recalibration took few seconds and introduced artefacts which were detected and corrected by interpolation. All the time series were resampled at 4 Hz and RRV and SAPV signals were obtained by high–pass filtering the corresponding series with a cut–off frequency of 0.03 Hz.

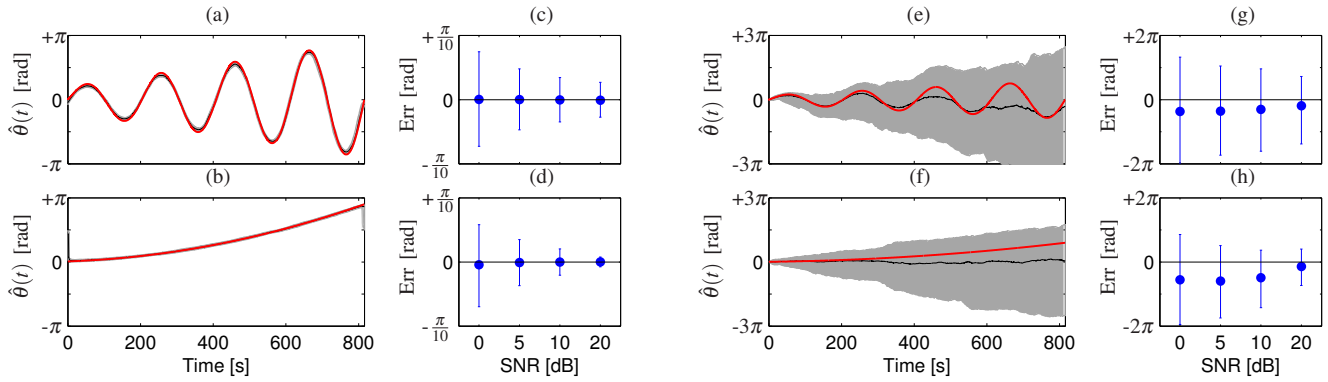


Fig. 2. Simulation studies. (a)–(d): results of the proposed methodology based on cross TF analysis; (e)–(h): results obtained by instantaneous frequency estimates. (a)–(b) and (e)–(f): red lines represent  $\theta(t)$ , while shadowed areas represent the range between the lower and upper quartile of estimates  $\hat{\theta}(t)$ . In these examples SNR=10 dB; (c)–(d) and (g)–(h): circles and bars represent the average of the I, II and III quartiles of the estimation errors. Note that the scales of the graphics are different.

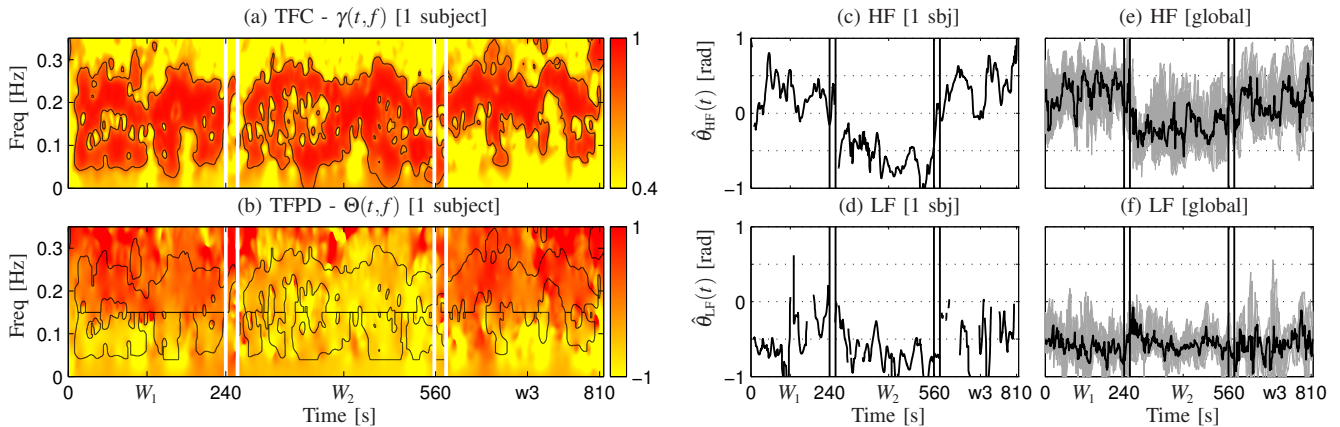


Fig. 3. Phase differences between RRV and SAPV during tilt table test. Vertical lines mark the early supine position, the head-up tilt and the later supine position. (a)–(d): Results from a subject. (e)–(f): Global results. (a): black contours encircled the regions where the TFC was statistically significant. (b): black contours represent  $\Omega_B$ . (c)–(d) phase differences estimated by averaging  $\Theta(t, f)$  in  $\Omega_B$ . (e)–(f) Global trends: lines represent the median values and the shadowed area the interval between the lower and upper quartile.

## IV. RESULTS

### A. Simulation studies

Time–frequency spectra were estimated by using the kernel of type (5), which gave a time and frequency resolution of about 12 s and 0.04 Hz. In the simulations, from each one of the 14 RRV signals, 50 couples of modified signals were generated for every SNR level. Given that  $\theta_{LF}(t) = \theta_{HF}(t)$ , the time course of  $\hat{\theta}(t)$  was obtained by averaging between  $\hat{\theta}_{LF}(t)$  and  $\hat{\theta}_{HF}(t)$ . The results are summarized in Fig. 2, where panels (a)–(d) and (e)–(h) show the results obtained by cross TF analysis as in (9) and by integration of the differences of the instantaneous frequencies, as in (2), respectively. Instantaneous frequencies were estimated as the frequencies corresponding to the maximum of the instantaneous auto TF spectra in both LF and HF bands. The time–courses of the estimated phase differences,  $\hat{\theta}(t)$ , are shown in panels (a)–(b) and (e)–(f), where results are given as the range between the lower and upper quartiles of the estimates. As shown, the estimator based on cross TF analysis was able to accurately track the changes of the phase differences in

both the considered cases, while the estimator based on the estimation of the instantaneous frequencies did not provide a reliable characterization of these changes. To quantify the goodness of the estimation, the median, and the lower and upper quartiles of the estimation errors,  $\theta_B(t) - \hat{\theta}_B(t)$ , were calculated for every iteration. The results of error analysis are given in Fig. 2c–d and Fig. 2g–h, where circles and bars represent the average of the median and of the interquartile ranges of the estimation errors. It is shown that the median errors were always lower than 0.01 rad, even for SNR as low as 0 dB. The variability of the estimation depended on the SNR and on the rate of variation of  $\theta(t)$ . For SNR=20 dB and for  $\theta(t)$  varying quadratically, the interquartile ranges were lower than 0.05 rad, less than 2% of the total range of variation of  $\theta(t)$ . While for SNR=0 dB and for  $\theta(t)$  varying sinusoidally, the interquartile range was about 0.4 rad, less than 10% of the total range of variation of  $\theta(t)$ . The estimation of the phase differences by integration of the differences between the instantaneous frequencies gave results characterized by much lower accuracy. The estimation errors were characterized by interquartile ranges at least 20

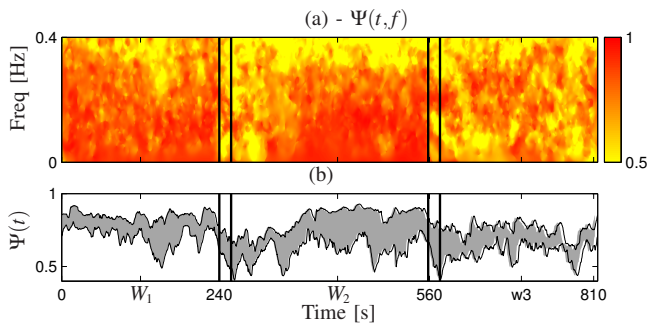


Fig. 4. (a): Time–frequency phase locking,  $\Psi(t,f)$ , between the RRV and SAPV estimated in 14 subjects undergoing tilt table test. (b): Interval between the I and III quartiles of  $\Psi(t,f)$ , estimated in  $f \in [0.04, 0.4]$  Hz.

times higher than those obtained by cross TF analysis (scales of Fig. 2g-h are 20 times higher than those of Fig. 2c-d). The impossibility of reliably estimating the phase differences by (2) was due to the difficulty of perfectly tracking the instantaneous frequencies of real signals, specially in HF band.

### B. Physiological study

An illustrative example of the estimation of the phase differences between the RRV and SAPV signals is shown in Fig. 3: despite the non–stationary structure of the signals, by TF coherence analysis was possible to localize regions in which coherence was statistically significant (see panel (a)). These regions, those for which  $M(t,f)=1$ , are encircled by a black contour. In Fig. 3b it is shown that the TFPD spectrum was negative in LF during the entire test and in HF during head-up tilt, thus indicating that in these TF regions SAPV led RRV signal. Parameters  $\hat{\theta}_{LF}(t)$  and  $\hat{\theta}_{HF}(t)$  were estimated by averaging the TFPD in  $\Omega_{LF}$  and  $\Omega_{HF}$ , whose boundaries are plotted as black contour. Too small regions for which  $M(t,f)=1$ , see Fig. 3a, were discarded from  $\Omega_B$ , see Fig. 3b, by the opening (8). In Fig. 3c, it is shown that for this subject, the movement back and forth from supine position to head–up tilt provoked almost instantaneous changes in  $\hat{\theta}_{HF}(t)$ , which during tilt decreased of about 0.85 rad and then, when supine position was restored, went back to values similar to those observed in early supine position. Results concerning the global trends of the study population are shown in Fig. 3e–f, where lines represent the instantaneous median values of  $\hat{\theta}_B(t)$  and shadowed areas the lower and upper quartiles, estimated among subjects. In this study population, the head–up tilt caused the phase differences to change in HF. The median trend of  $\hat{\theta}_{HF}(t)$  was  $0.29 \pm 0.18$  rad in  $W_1$ ,  $-0.20 \pm 0.14$  rad  $W_2$ ,  $0.15 \pm 0.17$  rad in  $W_3$ . The median trend of  $\hat{\theta}_{LF}(t)$  was  $-0.61 \pm 0.10$  rad in  $W_1$ ,  $-0.56 \pm 0.09$  rad in  $W_2$ ,  $-0.56 \pm 0.14$  rad  $W_3$ . On average, during the head–up tilt the time delay increased 361 ms in HF ranges, while it almost did not change in LF range.

The TFPL, shown in Fig. 4a, was high in large portions of the TF domain, especially during the second half of  $W_2$ . In Fig. 4b, the median trend and the interquartile range of the TFPL, evaluated for  $f \in [0.04, 0.4]$  Hz, is shown. The phase–locking,

whose median trend was  $0.73 \pm 0.09$ , quickly decreased after the beginning of the head–up tilt. About one minute after, the TFPL increased again, reaching values close to 0.85 about 2 minutes later.

## V. DISCUSSION

In this study, a new methodology for the quantification of phase differences in non–stationary cardiovascular signals, based on cross TF analysis, is proposed. Some of the advantages of this methodology are: the SPWVD provides auto and cross spectra characterized by high joint TF resolution; the localization of TF regions where spectral coherence is statistically significant (i.e., where the spectral components of two signals are sharing similar instantaneous frequencies) and where phase differences can be robustly estimated; the opening performed in (8) determines the minimum size of the TF regions which compose  $\Omega_B$ , thus adding robustness to the final estimates. In non–stationary context, this methodology was shown to provide accurate estimates also in presence of noise, and it outperformed techniques based on instantaneous frequency estimates. Finally, the TF representation of the phase–locking between different couples of signals allows to assess whether a determined stimulus provokes, among different subjects, similar patterns of synchronization. The analysis of signals recorded during tilt table test shows that head–up tilt provoked changes in the phase differences between RRV and SAPV. Moreover, the time–frequency representation of the phase locking among the subjects, which decreased immediately after the head–up tilt, was restored in about 2 minutes. This may suggest the existence of a common pattern of response to the orthostatic stress provoked by head–up tilt. The presented methodology provides a characterization of cardiovascular interactions which can add valuable information toward a better understanding of the dynamics involved in the cardiovascular control.

## REFERENCES

- [1] S. Aviyente, E. M. Bernat, W. S. Evans, and S. R. Sponheim, “A phase synchrony measure for quantifying dynamic functional integration in the brain.” *Hum Brain Mapp*, pp. 80–93, Mar 2010.
- [2] J.-P. Lachaux, A. Lutz, D. Rudrauf, D. Cosmelli, M. L. V. Quyen, J. Martinerie, and F. Varela, “Estimating the time-course of coherence between single-trial brain signals: an introduction to wavelet coherence.” *Neurophysiol Clin*, vol. 32, no. 3, pp. 157–174, Jun 2002.
- [3] Y.-J. Shin, D. Gobert, S.-H. Sung, E. J. Powers, and J. B. Park, “Application of cross time-frequency analysis to postural sway behavior: the effects of aging and visual systems.” *IEEE Trans Biomed Eng*, vol. 52, no. 5, pp. 859–868, May 2005.
- [4] F. Hlawatsch and G. F. Boudreaux-Bartels, “Linear and quadratic time-frequency signal representations,” *Signal Processing Magazine, IEEE*, vol. 9, no. 2, pp. 21–67, April 1992.
- [5] M. Orini, R. Bailón, L. T. Mainardi, A. Mincholé, and P. Laguna, “Continuous quantification of spectral coherence using quadratic time-frequency distributions: Error analysis and application,” in *Proc. Computers in Cardiology*, 2009, pp. 681–684.
- [6] E. Gil, M. Orini, R. Bailón, J. M. Vergara, L. Mainardi, and P. Laguna, “Photoplethysmography pulse rate variability as a surrogate measurement of heart rate variability during non-stationary conditions.” *Physiol Meas*, vol. 31, no. 9, pp. 1271–1290, Sep 2010.
- [7] M. Orini, L. T. Mainardi, E. Gil, P. Laguna, and R. bailón, “Dynamic assessment of spontaneous baroreflex sensitivity by means of time-frequency analysis using either rr or pulse interval variability.” *Conf Proc IEEE Eng Med Biol Soc*, vol. 1, pp. 1630–1633, 2010.